Single-band Hubbard model for the transport properties in bistable organic/metal nanoparticle/organic devices

Jianhua Wu, Liping Ma, and Yang Yang*

Department of Materials Science and Engineering, University of California at Los Angeles, Los Angeles, California 90095, USA

The transport properties of bistable organic/metal nanoparticle/organic devices are investigated within the single-band Hubbard model. The effect of two electrodes on the molecules with the nanoparticles is taken into account by using the Newns' chemisorption theory. The Coulomb interactions between the electrons in the Hubbard model are treated by the spectral density approach. The transmission probabilities of the system are calculated as a function of the energy, the organic layers' thickness, and the hopping term for the organic layers. At small bias, the transmission probability is small near the Fermi level if no charges are trapped in the system, which corresponds to the low-conductance state of the device. Above a threshold bias, the electrons within the nanoparticles will tunnel resonantly from one side to the other side, and the resulting positive-negative charges are trapped at both sides of the nanoparticle layer, in which case the transmission probability increases tremendously near the Fermi level, resulting in the high-conductance state. The layer-dependent densities of states are used to investigate the phenomena in detail. The transmission probability decreases exponentially as the thickness of the organic layers increases.

I. INTRODUCTION

In recent years, the electrical transport properties between two electrodes through an organic molecular layer have attracted a lot of attention both in experiment and in theory[1–22] It was first suggested by Aviram and Ratner,[1] that such a system should have the ability to rectify current. Recent experiments on molecular wires have included the studies of conduction in molecular thin films,[2,3] in the self-assembled monolayers using scanning tunnel microscopy,[4–8] and in single molecules that are connected between the tips of a mechanically controlled break junction.[9] Memory phenomena and devices are one of the most interesting phenomena in organic materials, and have been widely studied in the past years.[22–28] However, the organic bistable phenomenon has been found to be unreliable for long-term operations. Recently, a significant improvement was achieved when an ultrathin metal nanocluster layer is embedded between two organic layers. The resulting structure shows a unique electrical bistable behavior.[29–31] This device is defined as organic bistable device (OBD). The typical structure of an OBD consists of an organic/metal/organic trilayer structure interposed between an anode and a cathode.[29–31] When applying a low bias, there exist two stable conducting states. The high-conductance state (ON state) and the low-conductance state (OFF state) differ in their conductivities by several orders in magnitude and show remarkable retention. Once the device reaches either states, it tends to remain in that state for a prolonged period of time, and can be switched back and forth by applying a forward voltage pulse and a reverse voltage pulse.

The typical current-voltage curve from the experimental results is shown in Fig. 1. For the first bias ramping, the current injection of the device is very low initially and the device shows the OFF state. When the applied voltage (Φ) is over a critical value (Φ_{sw}), the device switches to the ON

state. For the second bias running, the device remains at the ON state. The ON state can be erased to the OFF state by applying a small reverse bias.[31] Therefore the device can be electrically programmed for nonvolatile memory applications.

Various interpretations of the bistable phenomena have been proposed in the past,[22–28] such as the transition from an amorphous state to a more long-range ordered state, the overlapping of the tails of the conduction and valence bands, and the formation of a metal bridge between the electrodes.[24] The internal rotation of the individual molecular complexes was proposed in Ref. 28. However, the performance of our OBDs is sensitive to the components of the middle metal layer.[29] This middle layer must have a nanoparticle structure. There exists a critical thickness for the nanoparticle layer, above which the bistable phenomenon appears, while below it the bistable phenomenon disappears.[29] The conductance transition was considered as a result of the charge redistribution in
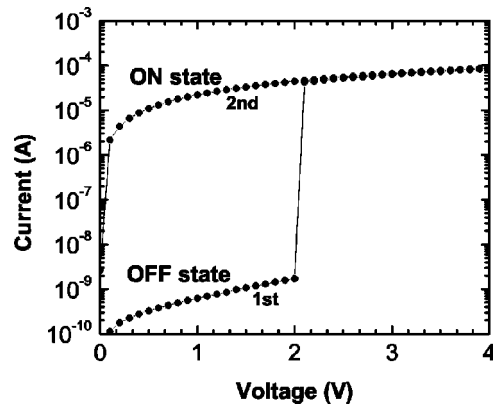

FIG. 1. The typical *I-V* curve for our OBD device measured experimentally. The film is an Al (80 nm electrode)/AIDCN (40 nm)/Al (20 nm)/AIDCN (40 nm)/Al (80 nm electrode) structure. Here AIDCN stands for 2-amino-4, 5-imidazoledicarbonitrite.

the middle nanoparticle layer in Ref. 29. It was shown by some experiments that the charge transfers from one side to the other side in nanoparticles forming a positive-negative electronic region. However, there is still a lack of theoretical understanding for the interpretation, and how this redistribution of the charge occurs is not clear. In the present paper, we propose a theoretical approach to the mechanism of the OBD's.

We refer to the electrode/organic/metal nanoparticles/ organic/electrode system as a one-dimensional structure. The total number of the organic molecules and the nanoparticles is N. Here the number of two organic molecules are d_{o1} and d_{o2}, respectively, and the number of the nanoparticles is d_n. Thus $N = d_{o1} + d_{o2} + d_n$. The Hubbard model is used here to study the organic molecules and the nanoparticles.[33,34] In the Hubbard model, each site represents an organic molecule or a nanoparticle. The interaction between two nearest-neighbor sites t_{ij} is determined by the hopping term. We consider a weak interaction between nearest-neighbor sites, that is, t_{ij} is much smaller than the on-site Coulomb interaction $U(i)$. The strong Coulomb interaction between the electrons causes the energy band to split into a higher- and a lower-energy subband. These two subbands are separated by an energy amount of the order of $U(i)$. Thus there is an energy gap in the nanoparticles, its value being equal to the on-site Coulomb interaction of the nanoparticles U_n. This separation of energy band is caused by the quantum effect of the nanoparticles. Without the applied bias, the system is in the non-charged state. The lower subband of nanoparticles is fully occupied, while the upper subband is empty. As the applied bias increases, the energy of the nanoparticles close to the anode will decrease due to the applied electrostatic potential, while that of those close to the cathode will increase. As a result, the energy of the lower subband of the nanoparticles close to the cathode will match the energy of the upper subband of the nanoparticle close to the anode. The electrons will tunnel resonantly from the lower subband in one nano-particle to the upper subband in the other nanoparticle with the same energy, forming partial occupied states—charged states, which are responsible for the ON state. This is similar to the treatment with hopping conductivity in granular metals.[32] The switch-on voltage is the voltage that makes the difference of electrostatic potentials between nearest-neighbor nanoparticles E_c equal to the energy gap between these two nanoparticles. As the bias increases further, the system is still in the charged state. When the applied bias decreases, the electrons in the upper subband of one nano-particle should hop to the lower subband of nearest-neighbor nanoparticle. However, due to the high barrier between the two nanoparticles originating from the native insulator coatings,[29] the trapped charges are still there when the bias is off. This is the nonvolatile memory behavior of OBD's.

The Hubbard model was originally introduced to explain band magnetism in transition metals, and it has become a standard model to study the essential physics of strongly correlated electron systems over the years. It was also used to explain the current-voltage characteristics of molecular wires.[20,35] This model, though in principle is rather simple, it provokes a nontrivial many-body problem that could be
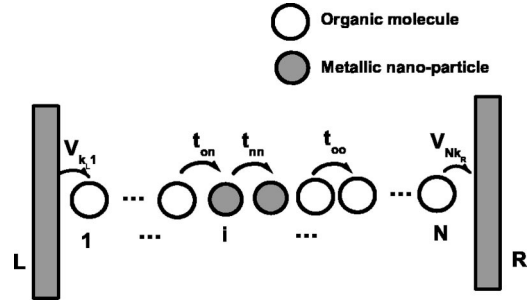

FIG. 2. The schematic diagram of the structure of ODB for calculation. L,R represent the left and the right electrodes, respectively. t_{on}, t_{nn}, t_{oo} are the hopping terms explained in the text. $V_{k_L 1}$ and $V_{N k_R}$ are the interactions between the electrodes and the organic molecules.

solved only for some special cases.[36–42] Thus we require an approximation scheme, which is simple enough to allow an extended study of electronic correlations. On the other hand, it should be clearly beyond Hartree-Fock (Stoner) theory, since we believe a reasonable treatment of the electron correlation effects to be vital for a proper description of electrical properties especially for nonzero temperatures. In this paper we use the spectral density approach[43,44] (SDA) to deal with the Hubbard model. The SDA, which reproduces the exact results of Harris and Lange[45] which concern the general shape of the spectral density in the strong-coupling limit $[U(i) \gg W$, W: bandwidth of the Bloch density of states], leads to a rather convincing result concerning the Hubbard model.[43,44,46] By comparison with different approximation schemes for the Hubbard model as well as numerically exact quantum Monte Carlo calculations in the limit of infinite dimensions, it showed[47] that the correct inclusion of the exact results of Harris and Lange[45] in strong-coupling regime is vital for a reasonable description of the properties of the Hubbard model.

The paper is organized as follows. The Hamiltonian of our model is proposed in Sec. II followed by description of our calculation of electrical current in Sec. III. In Sec. IV the solution for the Green function is presented with the treatment of the partition technique and with SDA. The results of the numerical evaluation of the theory and the discussions on the electrical behavior of the OBD systems are given in Sec. V. Finally, a summary is given.

II. THE HAMILTONIAN OF THE SYSTEM

We consider a one-dimensional system including two electrodes, organic molecules, and metal nanoparticles (Fig. 2). According to recent experimental results,[48] the metal nanoparticles were represented as metal nanoparticle cores coated with organic molecules or oxides. This is important in our theory, because as one can already see, the charge redistribution in the nanoparticles is the origin of the bistable memory.

The Hamiltonian of the system can be written as

$$\mathcal{H} = \mathcal{H}_0 + V, \tag{1}$$

where $\mathcal{H}_0$ is the Hamiltonian for the noninteracting parts (left and right electrodes, the organic molecules, and the metal nanoparticles), and V is the interaction between the electrodes and the organic molecules. The noninteracting Hamiltonian $\mathcal{H}_0$ is given as

$$\mathcal{H}_0 = \mathcal{H}_E + \mathcal{H}_{MN}, \tag{2}$$

where

$$\mathcal{H}_E = \sum_{P \in L,R} \sum_{k_P,\sigma} \epsilon_{k_P,\sigma} a^+_{k_P,\sigma} a_{k_P,\sigma} \tag{3}$$

is the Hamiltonian of the left and right electrodes, $a^+_{k_P,\sigma}$ ($a_{k_P,\sigma}$) is the creation (annihilation) operator for an electron with spin σ and energy $\epsilon_{k_P,\sigma}$, and k is the wave vector.

We use the Hubbard Hamiltonian to study the organic molecules with the metal nanoparticles,

$$\mathcal{H}_{MN} = \sum_{i,j,\sigma} (t_{ij} - t_{0i}\delta_{ij}) c^+_{i\sigma} c_{j\sigma} + \frac{1}{2} \sum_{i,\sigma} U(i) n_{i\sigma} n_{i,-\sigma}, \tag{4}$$

where $c^+_{i\sigma}$ ($c_{i\sigma}$) is the creation (annihilation) operator for an electron with spin σ at the site i for the organic molecules or the metal nanoparticles. $n_{i\sigma} = c^+_{i\sigma} c_{i\sigma}$ is the number operator with spin σ at site i. $U(i)$ are the on-site Coulomb interactions for the organic molecules and the metal nanoparticles at site i. t_{ij} are the hopping terms between the electrons at nearest-neighbor sites. t_{0i} is the on-site hopping integral at site i.

$$V = \sum_{P \in R,L} \sum_{k_P,i,\sigma} V_{k_P i} a^+_{k_P,\sigma} c_{i,\sigma} + \text{H.c.} \tag{5}$$

is the interaction between the organic molecules and the electrodes. $V_{k_P i}$ ($P = L,R$) is the strength of the interaction between electrodes and the nearest molecules. We assume that the left electrode can only interact with the first molecule, while the right electrode interacts with the last molecule.

III. CALCULATION OF ELECTRICAL CURRENT

We consider the transport of electrons through the organic molecules with the metal nanoparticles by modeling it as a one-electron elastic-scattering problem. An electron incident from the left electrode with an energy E has a transmission probability $T(E)$ to scatter into the right electrode. In the system, we suppose that the coupling between the two electrodes is weak, therefore, we can use the Landauer formula[49] to calculate the transmitted current as a function of the bias voltage Φ,

$$I = \frac{e}{\pi\hbar} \int_0^\infty dE [f(E - e\Phi/2) - f(E + e\Phi/2)] T(E), \tag{6}$$

where $f(E)$ is the Fermi distribution. The energy difference in the Fermi function of the left and right electrodes comes

from the applied bias voltage Φ. $e > 0$ is the elementary charge. At zero temperature and in the limit $\Phi \to 0$

$$I = \frac{e^2}{\pi\hbar} T(E_F)\Phi, \tag{7}$$

where E_F is the Fermi level of the system. Therefore the transmission probability near the Fermi level is most important for the electrical current at zero temperature.

The transmission probability can be obtained from the scatting theory[50]

$$T(E) = 4\pi^2 \sum_{k_L,k_R} |T_{k_L,k_R}|^2 \delta(E - E_L)\delta(E - E_R), \tag{8}$$

where $T_{k_L,k_R} = \langle k_L | T | k_R \rangle$ is the transmission amplitude from a state k_L in the left electrode to a state k_R in the right electrode with energy E. E_L (E_R) is the energy of electrons in the left (right) electrode. T is an operator in the scattering theory. In the weak-coupling limit of the two electrodes, the T operator

$$T = V + VGV \tag{9}$$

is usually replaced by its second term only. The first "direct" term V vanishes because there is no direct interaction between the states of the left and right electrodes. $G(E) = (E - \mathcal{H} + i0^+)^{-1}$ is the Green function of the system. Thus we get

$$T(E) = 4\pi^2 |G_{1N}(E)|^2 \Gamma_L(E)\Gamma_R(E), \tag{10}$$

where $G_{1N}(E)$ is the $(1,N)$ element of the Green function of the system in a matrix representation. $\Gamma_P(E)$ ($P \in L,R$) is

$$\Gamma_P(E) = \sum_{k_P} V^2_{k_P i} \delta(E - E_P). \tag{11}$$

The summation is over all the eigenstates of the left and the right electrode.

IV. SOLUTION TO THE GREEN FUNCTION

The basic quantity to be calculated is the retarded single-electron Green function $G(E)$, which includes all relevant information about system. In the matrix representation with a basis including the two electrodes, the organic molecules, and the metal nanoparticles, the Green function is the inverse of an infinite matrix. The Hamiltonian matrix is also an infinite matrix. In Ref. 21, Mujica *et al.* have proved that the Hamiltonian matrix can be exactly mapped into a reduced matrix defined in the space of states of the molecular wire, hence of dimension $N \times N$. In our system, the infinite matrix of the Hamiltonian can be mapped into a $N \times N$ matrix of the organic molecules with the metal nanoparticles subspace. Let H_{MN} be the matrix of the Hamiltonian of the organic molecules with the metal nanoparticles, then the reduced Hamiltonian matrix of the system, $\bar{H}_{MN}$, differs from H_{MN} only in both the first and last diagonal elements, $(1,1)$ and (N,N), which are explicitly given by

$$(\bar{H}_{MN})_{11} = (H_{MN})_{11} - \Pi_1(E),$$

$$(\bar{H}_{MN})_{NN} = (H_{MN})_{NN} - \Pi_N(E), \quad (12)$$

where $\Pi_{1(N)}(E)$ is a self-energy contribution of the electrodes given by

$$\Pi_1(E) = \sum_{k_L} \frac{V_{k_L 1}^2}{E - E_L + i0^+} = \Lambda_L(E) - i\Delta_L(E). \quad (13)$$

In the Newns' chemisorption theory,[34] $\Lambda_L(E)$ and $\Delta_L(E)$ have the forms

$$\Lambda_L(E) = \begin{cases} \dfrac{2V_{k_L 1}^2}{\gamma^2} E, & \left|\dfrac{E}{\gamma}\right| < 1 \\[2mm] \dfrac{2V_{k_L 1}^2}{\gamma^2}(E + \sqrt{E^2 - \gamma^2}), & \dfrac{E}{\gamma} < -1 \\[2mm] \dfrac{2V_{k_L 1}^2}{\gamma^2}(E - \sqrt{E^2 - \gamma^2}), & \dfrac{E}{\gamma} > 1 \end{cases} \quad (14)$$

and

$$\Delta_L(E) = \begin{cases} \dfrac{2V_{k_L 1}^2}{\gamma^2}\sqrt{\gamma^2 - E^2}, & \left|\dfrac{E}{\gamma}\right| < 1 \\[2mm] 0, & \text{otherwise,} \end{cases} \quad (15)$$

where γ is half the electrodes energy bandwidth, and E is measured from the center of the energy band of the electrodes. The similar expression for Σ_R can be obtained.

After the partition technique solution, the problem of the Green function is reduced to solve the Green function of the organic molecules and the metal nanoparticles with additional self-energy terms of electrodes to the $(1,1)$ and (N,N) elements. Thus we only need to solve Green function of the Hubbard model. However, the Hubbard model is a nontrivial problem, it can be solved only in some special cases.[36–42] In this paper, we use spectral density approach to the Hubbard model, which leads to a rather convincing result. In the following, we give only a brief derivation of the SDA solution and refer the reader to previous papers for a detailed discussion[44,46,47,51].

The Green function can now be given as

$$G(E)$$

$$= \begin{pmatrix} \mathcal{E}_{1\sigma}(E) & t_{12} & 0 & \cdots & & 0 \\ t_{21} & \mathcal{E}_{2\sigma}(E) & t_{23} & & & \vdots \\ 0 & & \ddots & & & 0 \\ \vdots & & & & \mathcal{E}_{N-1\sigma}(E) & t_{N-1,N} \\ 0 & \cdots & 0 & & t_{N,N-1} & \mathcal{E}_{N\sigma}(E) \end{pmatrix}^{-1},$$

$$(16)$$

where $\mathcal{E}_{i\sigma}(E) = E - t_{0i} - \Sigma_{i\sigma}(E) + \Pi_i(E)\delta_{i1} + \Pi_i(E)\delta_{iN}$. $\Sigma_{i\sigma}(E)$ is the site-dependent electronic self-energy which incorporates all the effects of the electron correlations.

The key point of the SDA is to find a reasonable ansatz for the self-energy. Guided by the precise solvable atomic limit of vanishing hopping $(t_{ij} = 0)$ and by the findings of Harris and Lange[44] in the strong-coupling limit $[U(i)/t_{ij} \gg 1]$, a one-pole ansatz for the self-energy $\Sigma_{i\sigma}(E)$ can be motivated:[43,44,46,47,51]

$$\Sigma_{i\sigma}(E) = U(i)n_{i-\sigma}\frac{E - B_{i-\sigma}}{E - B_{i-\sigma} - U(i)(1 - n_{i-\sigma})}. \quad (17)$$

The self-energy depends on the spin-dependent occupation numbers $n_{i\sigma}$ and the so-called band shift $B_{i\sigma}$. The band occupation can be obtained from the imaginary part of the Green function,

$$n_{i\sigma} = -\frac{1}{\pi}\int_{-\infty}^{+\infty} dE\, f(E)\ \text{Im}\ G_{ii\sigma}(E). \quad (18)$$

The band shift $B_{i\sigma}$ consists of higher correlation functions:

$$B_{i\sigma} = t_{0i} + \frac{1}{n_{i\sigma}(1 - n_{i\sigma})}\sum_{j \neq i} t_{ij}\langle c_{i\sigma}^+ c_{j\sigma}(2n_{i-\sigma} - 1)\rangle. \quad (19)$$

Although $B_{i\sigma}$ consists of higher correlation functions, it can be expressed exactly via $\text{Im}\,G_{i\sigma}$ and $\Sigma_{i\sigma}(E)$:[43,44,46,47,51]

$$B_{i\sigma} = t_{oi} - \frac{1}{n_{i\sigma}(1 - n_{i\sigma})}\frac{1}{\pi\hbar}\int_{-\infty}^{+\infty} dE\, f(E)\left(\frac{2}{U(i)}\Sigma_{i\sigma}(E) - 1\right)$$

$$\times [E - \Sigma_{i\sigma}(E) - t_{oi}]\ \text{Im}\ G_{i\sigma}(E). \quad (20)$$

Now a closed set of equations for the Green function is established via Eqs. (16)–(18) and (20), which can be solved self-consistently.

V. RESULTS AND DISCUSSION

In our calculations, we keep the on-site Coulomb interaction in the organic molecules fixed at $U_o = 2.0$ eV. The on-site Coulomb interaction in the metal nanoparticles fixed at $U_n = 0.5$ eV.[52] The bandwidths of the two electrodes are $2\gamma = 10.0$ eV. The center of the energy band in the left electrode is located at $E_F - e\Phi/2$, and in the right electrode at $E_F + e\Phi/2$ due to the applied electrical bias Φ. The Fermi energy level is set to zero. The hopping terms between the organic molecules, between the metal nanoparticles, and between a molecule and a nanoparticle are set to be smaller than that used in the literature[20] for the conductance in molecular wires. Because the hopping term represents the overlapping between the nearest electrons, the electron hops intermolecularly in our system, while it happens intramolecularly in the molecular wires. It was shown that the conductance of molecular wires through the molecular overlapping is two orders smaller than through one molecule.[13] This means the hopping terms between nearest molecules are about one order smaller than between nearest atoms within a
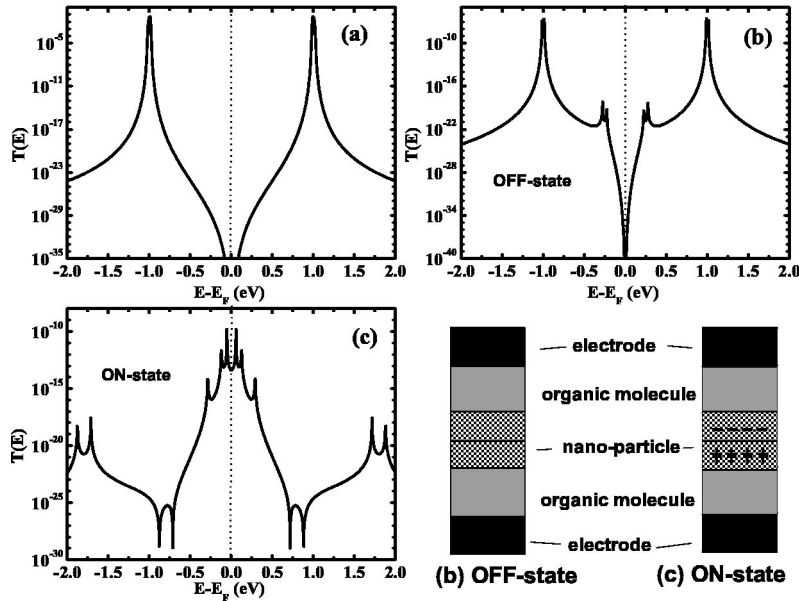
FIG. 3. The transmission probabilities $T(E)$ as a function of energy for the following cases: (a) pure six-layer organic molecular film; (b) 2/2/2 structure and without electron charge in nanoparticles $[n(3)=n(4)=1.0]$; (c) 2/2/2 structure with charge redistributed in the nanoparticle layer $[n(3)=1.4,n(4)=0.6]$. The schematic structures of the device for the OFF state and ON state are plotted at the right corner. Other parameters are $t_{oo}=t_{on}=0.025$ eV, $t_{nn}=0.05$ eV, $\Phi=0.0$ V, $T=50$ K, $V_{k_L1}=V_{Nk_R}=0.05$ eV, the band occupation of organic molecules is $n_o=1.0$.

molecule. In the following, the hopping term between the nearest organic molecules is defined as t_{oo}, the term between the nearest organic molecules and the metal nanoparticle as t_{on}, and the term between the nearest nanoparticles is t_{nn}. We will refer to the considered structure electrode/organic molecules/nanoparticles/organic molecules/electrode as $d_{o1}/d_n/d_{o2}$, where $d_o=d_{o1}=d_{o2}$.

It should be noted that the spatial profile of the electrostatic potential is not considered in our self-consistent calculation. Instead, we only calculate the spatial profile of the electrostatic potential in two supposed cases (charged and noncharged states). This profile will affect the local energy terms t_{0i}. On the other hand, the change of local energy terms will affect the distribution of the spatial concentration of the charges. These effects should be solved simultaneously with the coupling quantum mechanic equation and Poisson equation.[53,14] In our calculation, we fixed the band occupation for each site, and adjust the local energy term to fit the band occupation. In addition, we assume that the electrical neutral state is the state where each site has a band occupation of $n_i=1.0$. Thus the charged state refers to the state with $n_i \neq 1.0$ for any site. For the noncharged states, the band occupation of each site is $n_i=1.0$, the local energy for the organic molecules is set to $t_0=-1.0$ eV and that for the nanoparticles to $t_0=-0.25$ eV. The charged state is a metastable state; it cannot be obtained from the self-consistent solution of the Hamiltonian. There are two ways to get the charged states: the first one is fixing the Fermi energy for the whole system, and adjusting the local energy for each site to fit the band occupation of each site, which corresponds to adjusting the electrostatic potential of each site. The second one is fixing the local energy and adjusting the Fermi energy for each site. On the other hand, there may exist many self-consistent solutions for the Hamiltonian model, but here we are only interested in the nonmagnetic solution and calculate the self-consistent solution from a higher temperature to a lower temperature.

First, let us see the influence of the metal nanoparticles on

the properties of the organic molecular films. In Fig. 3, we plot the transmission probabilities as a function of energy for the cases with and without the nanoparticles. Without the nanoparticles [Fig. 3(a)], the transmission probability renders several peaks at the energy around $E=\pm 1.0$ eV. Because the Coulomb repulsion between the organic molecules is $U_o=2.0$ eV, the energy bands of the molecules are located around $E=\pm 1.0$ eV. For the other energy regimes, $T(E)$ is very small. When a thin metal nanoparticle layer is inserted into the organic layers [Figs. 3(b) and 3(c)], the transmission probabilities change significantly, especially for the case where electrons are redistributed in the metal nanoparticles (polarized state) [Fig. 3(c)]. For the noncharged state [Fig. 3(b)], two small additional peaks of $T(E)$ appear with the energies around $E=\pm 0.25$ eV, where the energies of the metal nanoparticle energy bands are located. Because the Fermi level is located in the gap between the two Hubbard subbands of the organic molecules and of the metal nanoparticles, the transmission probability is very small at the Fermi level. Therefore the conductance of the system is very small for the case without the metal nanoparticle layer, and the case with the metal nanoparticles at noncharged state. However, when the electrons are redistributed in the metal nanoparticles [Fig. 3(c)], the situation changes significantly. As one can see from Fig. 3(c), the charge in the metal nanoparticles plays an important role to determine the transmission probability, especially at the energy near the Fermi level. At the polarized state, $T(E)$ at the Fermi level becomes much higher than that of noncharged state. $T(E)$ exhibits some peaks at the energies around the Fermi level, which are corresponding to the energy bands of the metal nanoparticles. The peaks of $T(E)$ induced by the organic molecule energy bands shift to the energies farther from the Fermi energy ($E \sim \pm 1.8$ eV) in the polarized state compared to the noncharged state. This will induce large electrical current in the structure. As for the experimental I-V behavior shown in Fig. 1, for the first bias running from 0 to 4 V, the current is very low and increases slowly at bias below 2 V. The metal nano-
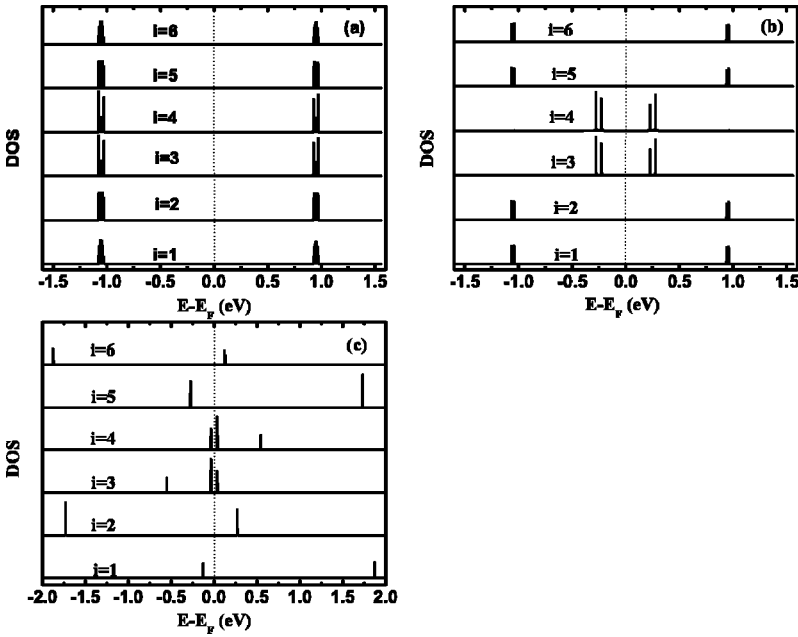
FIG. 4. The layer-dependent density of states as a function of energy for the same cases as in Fig. 3. All the parameters are the same as in Fig. 3.

particles will have no charges trapped in them. This is corresponding to the OFF state in Fig. 3(b). As the applied bias increases, the electrostatic potential for the electrons in the nanoparticles close to the anode will drop while that near the cathode will increase. At the threshold bias voltage (Φ_{sw}), the electrons at the metallic core of the nanoparticles close to the cathode will tunnel to the other side, forming the polarized state. This will result in the rapid increase of the electrical current in the system [from Fig. 3(b) to Fig. 3(c)]. When the bias decreases, this polarized state remains due to the barrier between nanoparticles, so the system remains in the ON state. We would like to point out that the ON state is a metastable state, and the charge is trapped in the nanoparticles. Thus there must exist a potential barrier between the two nanoparticles on both sides, so that the charges can be stored in the nanoparticles. This is exactly what the experiment shows, because in our recent experiments, the memory phenomenon only appears for the case where the middle metal nanoparticles were coated with the organic molecules or oxides.

However, the same-kind charge trapping in the nanoparticles might also occur through charge injection from the electrodes. The transmission probability $T(E)$ may also increase tremendously near the Fermi level in this case.[54] From the experimental results,[29] we think that the mechanism of our OBD device can be explained by the charge redistribution in the nanoparticles. First, the ON state can be erased only by a small negative bias. For the same-kind charge trapping in the nanoparticles, the system will be symmetrical. Therefore, a small positive as well as a small negative bias will erase the ON state. However, this is not found in our experiments. Second, if the bistable phenomenon is caused by the same-kind charge trapping in the nanoparticles, the switching voltage may depend on the scanning speed of the applied voltage. In our experiments, the same switching voltage is observed for different scanning speeds of the applied voltage. Third, the switching voltage is independent of the

temperature[55] which indicates a tunneling process for charge redistribution, rather than a charge injection-trapping process, which is thermally active. Finally, the switching speed of the OBD is in nanoseconds range, which also supports the argument that the charge redistribution occurs by resonant tunneling within the nanoparticles, rather than by the same-kind charge injection trapping.

The layer-dependent density of states (DOS) is shown in Fig. 4 for the same cases as in Fig. 3. The strong Coulomb interaction between the electrons causes the spectrum to split into a high- and a low-energy subband ("Hubbard splitting"). These two subbands ("Hubbard bands") are separated by an energy amount of the order $U(i)$. In one-dimensional system, the upper and the lower subbands contain several isolated peaks. Without the hopping effect, the peaks will appear only at the energy levels of the upper (corresponding to the lowest unoccupied molecular orbit) and the lower (corresponding to the highest occupied molecular orbit) Hubbard subbands of the organic molecules and the eigenvalues of metal nanoparticles. Due to the hopping effect, each peak splits into several little peaks. In the case of charged state [Fig. 4(c)], the peaks of the DOS in the metal nanoparticles ($i=3,4$) shift in a different way. The resultant peaks of the DOS in the organic molecules ($i=1,2,5,6$) also shift in different ways. Thus there exist several peaks around the Fermi level. This is the reason why $T(E)$ is much higher around Fermi energy in this case.

In order to see the spatial distribution of the electrostatic potential, we calculated the electrostatic potential for non-charged and charged states at different applied bias (Fig. 5). We do not consider the potential drop at the interface between the electrode and the organic layers. The dielectric constant for the nanoparticles is chosen to be 2.0 as an average. The structure is substrate/Al (80 nm)/organic layer (40 nm)/middle layer (20 nm)/organic layer (40 nm)/Al (80 nm) which is the typical structure in our experiments. We assume that there are two nanoparticles in the middle metal layer,
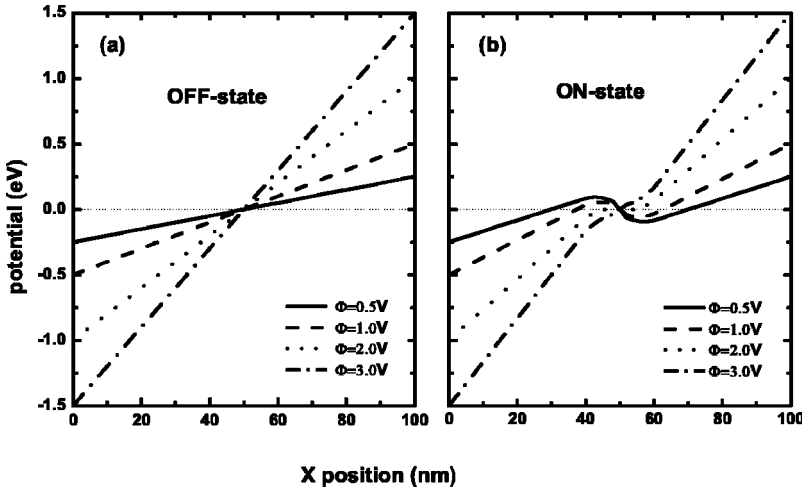
FIG. 5. The electrostatic potential for non-charged and charged states of the structure substrate/Al (80 nm)/organic layer (40 nm)/middle layer (20 nm)/organic layer (40 nm)/Al (80 nm) for different applied bias Φ. There are two nanoparticles in the middle nanoparticle layer. (a) Noncharged state (OFF state); (b) charged state (ON state), the charge in the two nanoparticles is $q_1 = -0.4e, q_2 = 0.4e$ which is the same as the parameters in Fig. 3. The x axis is measured from left organic layer to the right organic layer.

and the charge distributes evenly in the nanoparticles. The diameters of the nanoparticles are 6 nm. The distance between the centers of neighboring nanoparticles is $d_{nn} = 14$ nm. The potential at center of the system is set to zero, therefore the potentials at the left and the right electrodes are $\pm e\Phi/2$ which depend on the position of anode and cathode. We assume that the left electrode is the anode. Thus the potential at the left electrode is $-e\Phi/2 < 0$, and at the right electrode is $e\Phi/2 > 0$. It is apparent that the potential increases linearly from the left to the right electrodes in the noncharged states. As we mentioned in the itroduction, the switching voltage is the voltage which makes the difference of electrostatic potential between the nearest-neighbor nanoparticles equal to the gap of the energy level of nanoparticles. In our case, the energy gap of nanoparticles is $U_n = 0.5$ eV, which gives the switching voltage $\Phi_{sw} = (U_n/d_{nn})d_{tot}$ to be about 3.6 V (d_{tot} is the thickness of the system except the electrodes). It is in close agreement with our experimental results. The variation of experimentally measured switching voltage is due to the variation of the distance between nearest nanoparticles and the variation of the size of the nanoparticles. However, when the electrons redistribute in the nanoparticles, the electrostatic potential changes a lot. The potential drops slowly in the middle nano-

particle layer. The major drop of potential is across the organic molecular layers. Even at a very low bias, the potential will have a negative drop at the nanoparticles compared to the drop across the whole system. This results in the electrical potential drop across the organic molecular layers being larger than the applied bias.

Let us now turn our attention to the influence of the hopping term of the organic molecules on $T(E)$. The hopping dependence of $T(E_F)$ at Fermi level is plotted in Fig. 6. $T(E_F)$ increases quickly as the hopping term $t_{oo} = t_{on}$ increases at small t_{oo}. It will reach a saturation value as t_{oo} increases to a large value. This means that the increase of the overlap between the organic molecules will increase the conductance of the organic molecules and the nanoparticle system. This is because as the hopping increases, the electrons are easier to transmit through the regime of the organic molecules and the metal nanoparticles.

The effect of the thicknesses $d_{o1} = d_{o2} = d_o$ of the organic molecules on $T(E_F)$ is plotted in Fig. 7. As the thickness of the organic molecules increases, the resistance to scattering electrons increases too. Thus the transmission probability will decrease. One can see that $T(E_F)$ decreases exponentially as d_o increases. This is the same as the theoretical
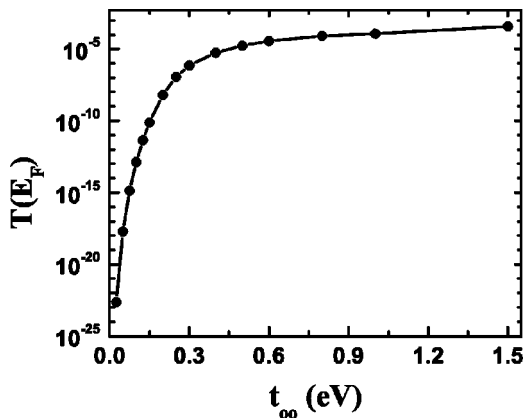

FIG. 6. The transmission probability $T(E_F)$ as a function of the hopping term t_{oo} in the case of different charge trapped in nanoparticles (ON state). Other parameters are the same as Fig. 3(c).
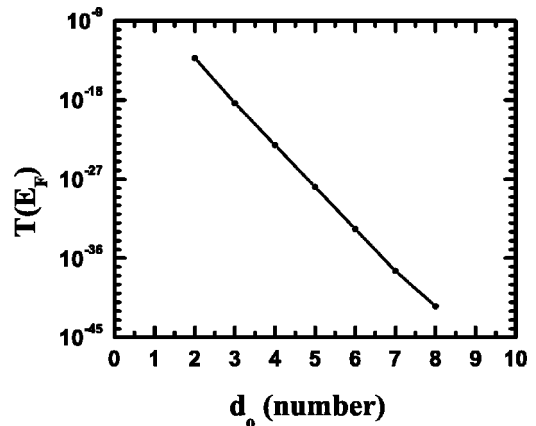

FIG. 7. The transmission probability $T(E_F)$ at the Fermi level as a function of the thicknesses $d_o = d_{o1} = d_{o2}$ of the organic molecules in the case of different charge trapped in the metal nanoparticles (ON state). Other parameters are the same as Fig. 3(c).

results obtained in the pure molecular wires in the case of the small hopping term.[17,21,16,56] This is because the hopping term is much smaller compared to the energy gaps of the molecules.

VI. SUMMARY

In this paper, we studied the transport properties of the organic bistable device. We think that the mechanism of the bistable phenomenon is caused by the charge redistribution in the nanoparticle layers. By the calculation of transmission probability, we find that the charge redistribution in the nanoparticles plays a very important role for the transport properties of the OBD. The transmission probability $T(E)$ increases tremendously near the Fermi level in the polarized state compared to the noncharged state.

The thickness and hopping effect on the transport properties are discussed in detail. The transmission probability decreases exponentially as the thickness of the organic molecules increases. The transmission probability will increase as the hopping term of the organic molecules increases. But the hopping dependence of the transmission probability is neither a linear one nor an exponential one.

ACKNOWLEDGMENTS

---

*Corresponding author. Email address: yangy@ucla.edu; URL: http://www.seas.ucla.edu/ms/faculty1/YYLab/yylabs.htm

[1] A. Aviram and M.A. Ratner, Chem. Phys. Lett. **29**, 257 (1974).

[2] C.M. Fischer, M. Burghard, S. Roth, and K. von Klitzing, Surf. Sci. **361/362**, 905 (1995).

[3] C. Zhou, M.R. Deshpande, M.A. Reed, L.J. Il, and J.H. Tour, Appl. Phys. Lett. **71**, 611 (1997).

[4] R.P. Andres, J.D. Bielefeld, J.I. Henderson, D.B. Janes, V.R. Kolagunta, C.P. Kubiak, W.J. Mahoney, and R.G. Osifchin, Science **273**, 1690 (1996).

[5] C.A. Mirkin, R.L. Letsinger, R.C. Micic, and J.J. Storhoff, Nature (London) **382**, 607 (1996).

[6] L.A. Bumm, J.J. Arnold, M.T. Cygan, T.D. Dunbar, T.P. Burgin, L. Jones II, D.L. Allara, J.M. Tour, and P.S. Weiss, Science **271**, 1705 (1996).

[7] B.C. Stipe, M.A. Rezaei, W. Ho, S. Gao, M. Persson, and B.I. Lundqvist, Phys. Rev. Lett. **78**, 4410 (1997).

[8] S. Datta, W. Tian, S. Hong, R. Reifenberger, J.I. Henderson, and C.P. Kubiak, Phys. Rev. Lett. **79**, 2530 (1997).

[9] M.A. Reed, C. Zhou, C.J. Muller, T.P. Burgin, and J.M. Tour, Science **278**, 252 (1997).

[10] M. Di Ventra, S.-G. Kim, S.T. Pantelides, and N.D. Lang, Phys. Rev. Lett. **86**, 288 (2001).

[11] N.B. Zhitenev, H. Meng, and Z. Bao, Phys. Rev. Lett. **88**, 226801 (2002).

[12] M. Di Ventra, S.T. Pantelides, and N.D. Lang, Phys. Rev. Lett. **88**, 046801 (2002).

[13] E.G. Emberly and G. Kirczenow, Phys. Rev. B **64**, 125318 (2001); **64**, 235412 (2001).

[14] A. Nitzan, M. Galperin, G.-L. Ingold, and H. Grabert, J. Chem. Phys. **117**, 10 837 (2002).

[15] M.P. Samanta, W. Tian, S. Datta, J.I. Henderson, and C.P. Kubiak, Phys. Rev. B **53**, R7626 (1996).

[16] M. Kemp, A. Roitberg, V. Mujica, T. Wanta, and M.A. Ratner, J. Phys. Chem. **100**, 8349 (1996).

[17] M. Magoga and C. Joachim, Phys. Rev. B **56**, 4722 (1997).

[18] S. Datta and W. Tian, Phys. Rev. B **55**, R1914 (1997).

[19] E. Emberly and G. Kirczenow, Ann. N.Y. Acad. Sci. **852**, 54 (1998).

[20] V. Mujica, M. Kemp, A. Roitberg, and M. Ratner, J. Chem. Phys. **104**, 7296 (1996).

[21] V. Mujica, M. Kemp, and M. Ratner, J. Chem. Phys. **101**, 6849 (1996); **101**, 6856 (1994).

[22] J. Chen, M.A. Reed, A.M. Rawlett, and J.M. Tour, Science **286**, 1550 (1999).

[23] H.K. Henish and W.R. Smith, Appl. Phys. Lett. **24**, 589 (1974).

[24] Y. Segui, B. Ai, and H. Carchano, J. Appl. Phys. **47**, 140 (1976).

[25] R.S. Potember, T.O. Poehler, and D.O. Cowan, Appl. Phys. Lett. **34**, 405 (1979).

[26] A. Aviram, C. Joachim, and M. Pomerantz, Chem. Phys. Lett. **146**, 490 (1988).

[27] R. Kumai, Y. Okimoto, and Y. Tokura, Science **284**, 1645 (1999).

[28] H.J. Gao, K. Sohlberg, Z.Q. Xue, H.Y. Chen, S.M. Hou, L.P. Ma, X.W. Fang, S.J. Pang, and S.J. Pennycook, Phys. Rev. Lett. **84**, 1780 (2000).

[29] L.P. Ma, S. Pyo, J.Y. Ouyang, Q.F. Xu, and Y. Yang, Appl. Phys. Lett. **82**, 1419 (2003).

[30] L.P. Ma, J. Liu, and Y. Yang, Appl. Phys. Lett. **80**, 2997 (2002).

[31] L.P. Ma, J. Liu, S. Pyo, and Y. Yang, Appl. Phys. Lett. **80**, 362 (2002).

[32] P. Sheng, B. Abeles, and Y. Arie, Phys. Rev. Lett. **31**, 44 (1973).

[33] J. Hubbard, Proc. R. Soc. London, Ser. A **276**, 238 (1963); **281**, 401 (1964).

[34] D.M. Newns, Phys. Rev. **178**, 1123 (1969).

[35] T. Kostyrko and B. Bulka, Phys. Rev. B **67**, 205331 (2003).

[36] E.H. Lieb and F.Y. Wu, Phys. Rev. Lett. **20**, 1445 (1968).

[37] F.D.M. Haldane, J. Phys. C **14**, 2585 (1981).

[38] V. Meden and K. Schöhammer, Phys. Rev. B **46**, 15 753 (1992).

[39] J. Voit, Rep. Prog. Phys. **58**, 977 (1995).

[40] W. Metzner and D. Vollhardt, Phys. Rev. Lett. **62**, 324 (1989).

[41] E. Müller-Hartmann, Int. J. Mod. Phys. B **3**, 2169 (1989).

[42] A. Georges, G. Kotliar, W. Krauth, and M.J. Rozenberg, Rev. Mod. Phys **68**, 13 (1996).

[43] W. Nolting and W. Borgiel, Phys. Rev. B **39**, 6962 (1989).

[44] T. Herrmann and W. Nolting, J. Magn. Magn. Mater. **170**, 253 (1997).

[45] A.B. Harris and Q.V. Lange, Phys. Rev. **157**, 295 (1967).

[46] M. Potthoff and W. Nolting, J. Phys.: Condens. Matter **8**, 4937 (1996).

[47] M. Potthoff, T. Herrmann, T. Wegner, and W. Nolting, Phys. Status Solidi B **210**, 199 (1998).

[48] The recent experiment results show that the middle layer must be nanoparticles coated by the organic molecules or oxides.

[49] R. Landauer, IBM J. Res. Dev. **1**, 223 (1957); Phys. Lett. **85A**, 91 (1981).

[50] A. Nitzan, Annu. Rev. Phys. Chem. **52**, 681 (2001).

[51] J.H. Wu, T. Herrmann, and W. Nolting, Phys. Rev. B **60**, 12 226 (1999).

[52] We use the electrostatics energy $e^2/2C$ (C is the capacitance of the nanoparticle) for the nanoparticle with an electron stored as the Coulomb repulsion in the metal nanoparticles. The capacitance of the nanoparticles is about 2.0 aF. See F.-R.F. Fan and A.J. Bard, Science **227**, 1791 (1997); D.C. Ralph, C.T. Black, and M. Tinkham, Phys. Rev. Lett. **74**, 3241 (1995).

[53] V. Mujica, A.E. Roitberg, and M.A. Ratner, J. Chem. Phys. **112**, 6834 (2000).

[54] The transmission probabilities $T(E)$ are also calculated as a function of energy for the case of the same kind of charges trapped in the nanoparticles. It shows that $T(E)$ also increases tremendously near the Fermi level.

[55] L.P. Ma, J. Liu, S. Pyo, Q.F. Xu, and Y. Yang, Mol. Cryst. Liq. Cryst. **378**, 185 (2002).

[56] M. Olson, Y. Mao, T. Windus, M. Kemp, M.A. Ratner, N. Léon, and V. Mujica, J. Phys. Chem. **102**, 941 (1998).